Supplementary Information

Kinetic Control of Perovskite Thin Film Morphology and Application in Printable Light Emitting Diodes.

Prashant Kumar[1], Baodan Zhao[2], Richard.H.Friend[2], Aditya Sadhanala[*,2] K.S.Narayan[*,1]

1. Jawaharlal Nehru Centre for Advanced Scientific Research, Bangalore, India -560064

2. Cavendish Laboratory, University of Cambridge, JJ Thomson Avenue, CB3 0HE Cambridge, UK

* Email: [*,1]narayan@jncasr.ac.in, *[,2]as2233@cam.ac.uk

I. Sheet like morphology in TPBi treated films

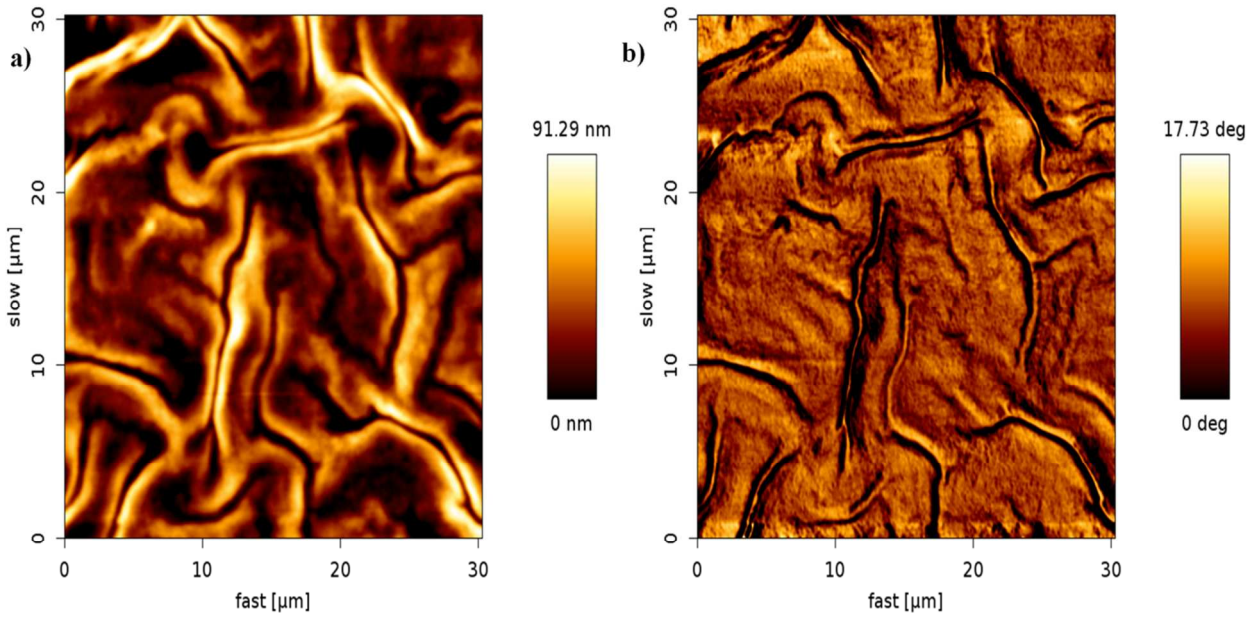

Figure S1: Sheet like wrinkled morphology observed in TPBi additive treated A-SMC films.

IIa. Photothermal deflection spectra (PDS) of perylene treated A-SMC films.

The Perylene treated film shows an additional peak as compared to the solvent only treated film. This additional peak can be attributed to the perylene absorption, which is evident from a good match between perylene only absorption with the observed peak in A-SMC absorption (figure S2).

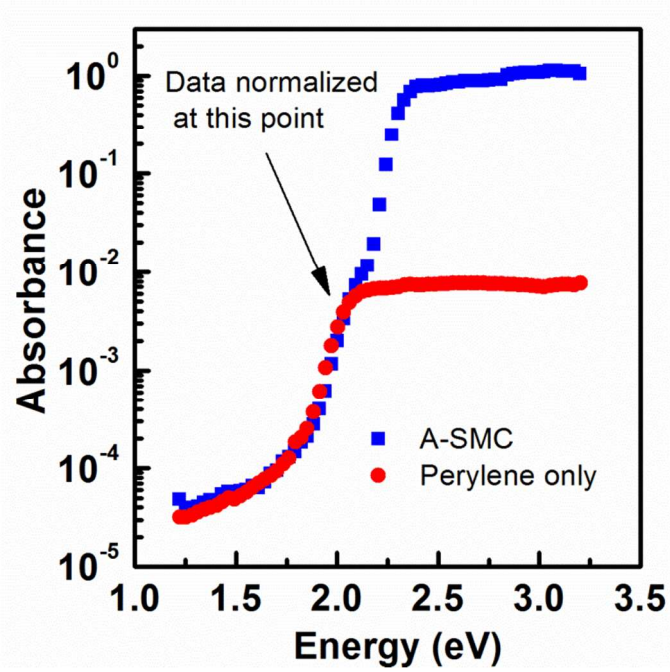

Figure S2. PDS absorbance spectra of perylene treated perovskite films (A-SMC) (blue, squares) and absorbance spectra of perylene only films (red circles).

IIb. PL lifetime measurements.

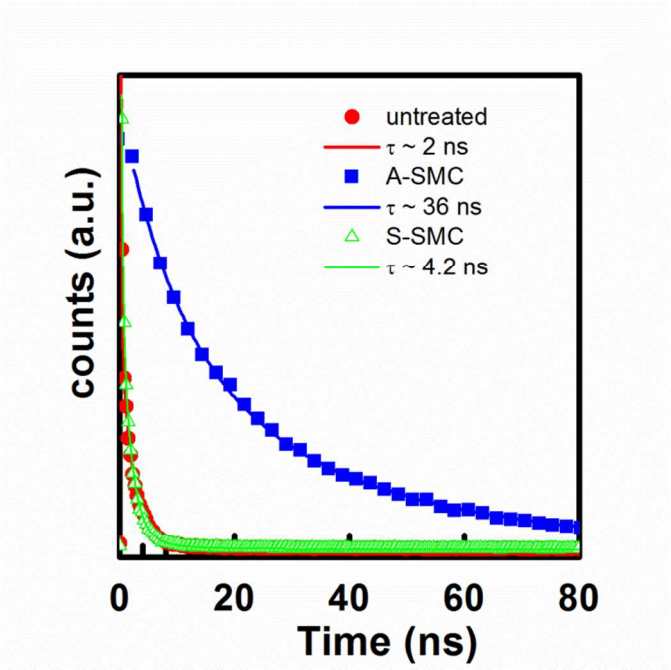

Figure S3. TCSPC lifetime measured for untreated films (red circles), S-SMC films (green circles) and PTCDA treated perovskite films (blue, squares).

IIIa. AFM and Confocal map of S-SMC thin films.

The morphology of solvent treated films appears to be very different as compared to perylene additive treated films. While the grain size is reduced and the coverage is more uniform, no significant microstructures are visible. Large scale morphology shows wrinkle formation, while the emission intensity is inhomogeneously distributed over the scan region. Figure S4a shows the AFM morphology of S-SMC films, which indicates that the grain sizes are larger than that of A-SMC. Figure S4b shows confocal emission scan of the S-SMC film.

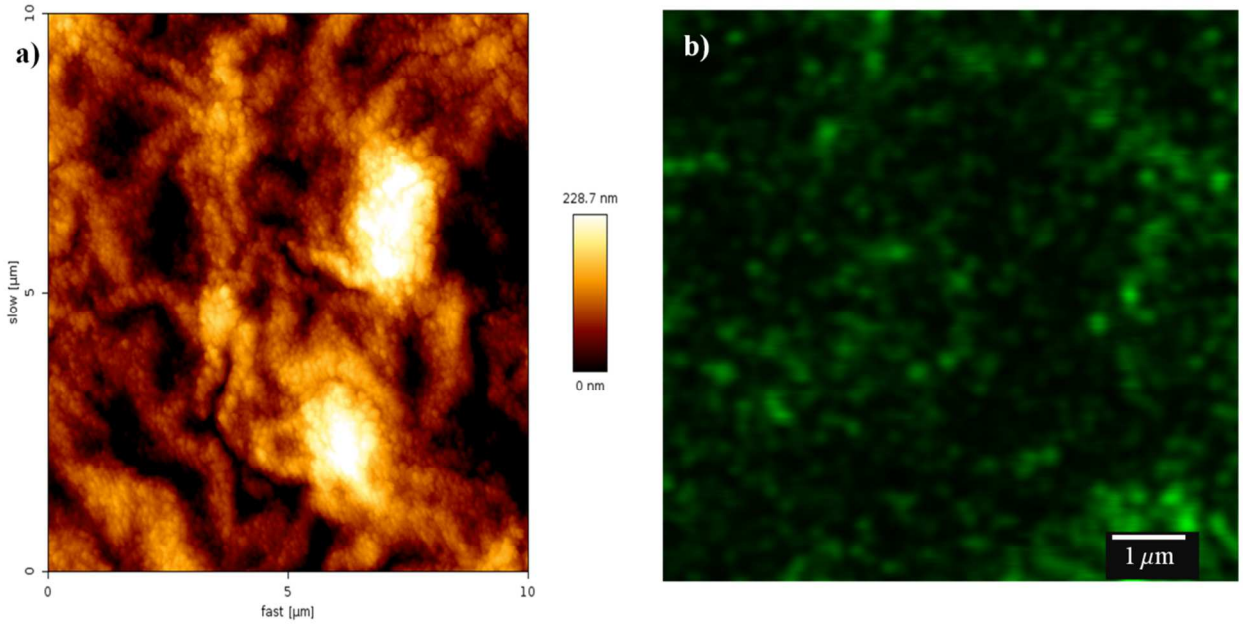

Figure S4: a) AFM morphology of S-SMC films, b) Confocal image map of S-SMC films.

IIIb. AFM and confocal map of A-SMC films post heat treatment.

The large scale micro-structures observed in A-SMC films tend to smear out upon annealing (5 min at 100 ^{o}C). The morphology is more homogeneous with the lack of any structuring as is shown in figure S5a; the emission intensity is uniformly distributed over the entire scan region (figure S5b).

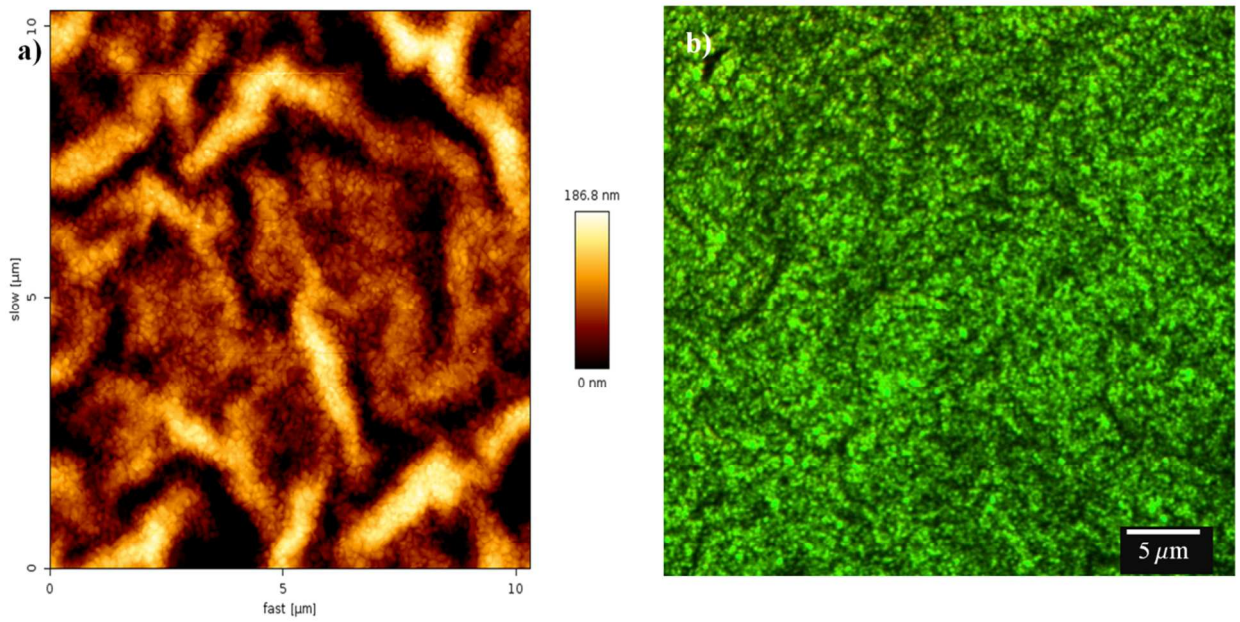

Figure S5. a) AFM topography of A-SMC films post annealing, b) Confocal emission of A-SMC films post annealing.

IVa. Alloy electrode charesteristics.

The vacuum free, low temperature melting back contact forms uniform contact with the TPBi layer on top of OIP. The SEM micrograph shown in figure S6a suggests low surface roughness. The elemental analysis performed using EDAX shows all the constituents to be presented at the interface, contributing towards the work function (figure S6b).

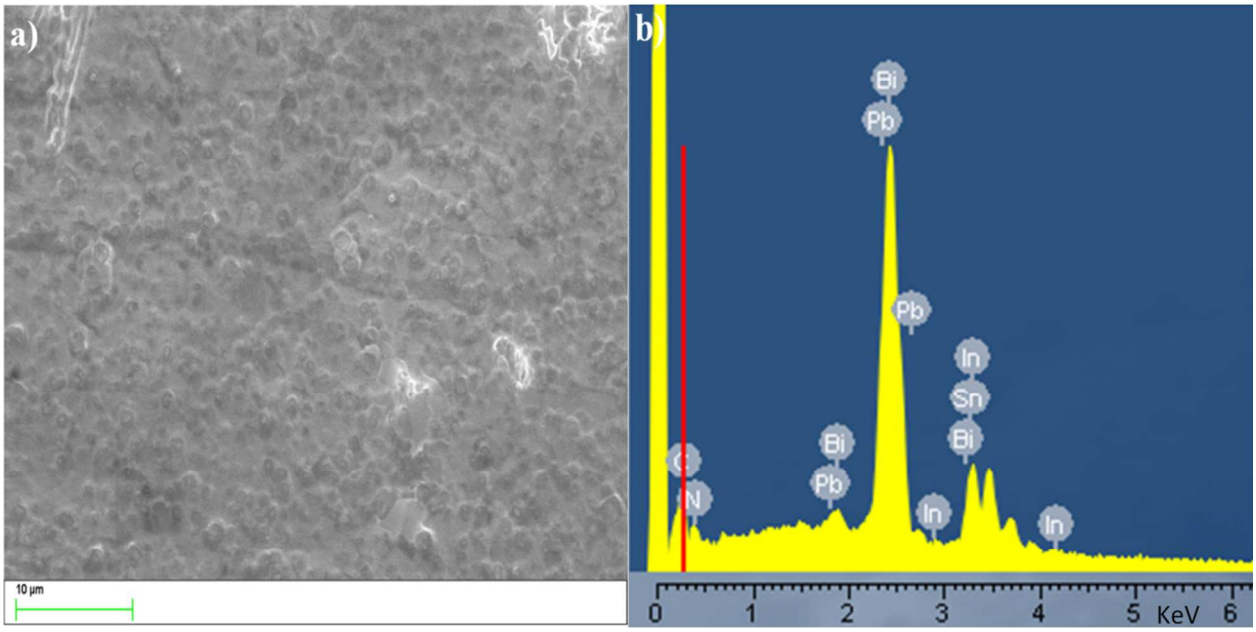

Figure S6: a) SEM map of alloy electrode in contact with TPBi layer (measured after cleaning with chloroform), b) EDAX elemental map shows presence of Bi, Sn, In, and Pb at the interface.

IVb. Work function estimation using Ultraviolet photo-electron spectroscopy (UPS).

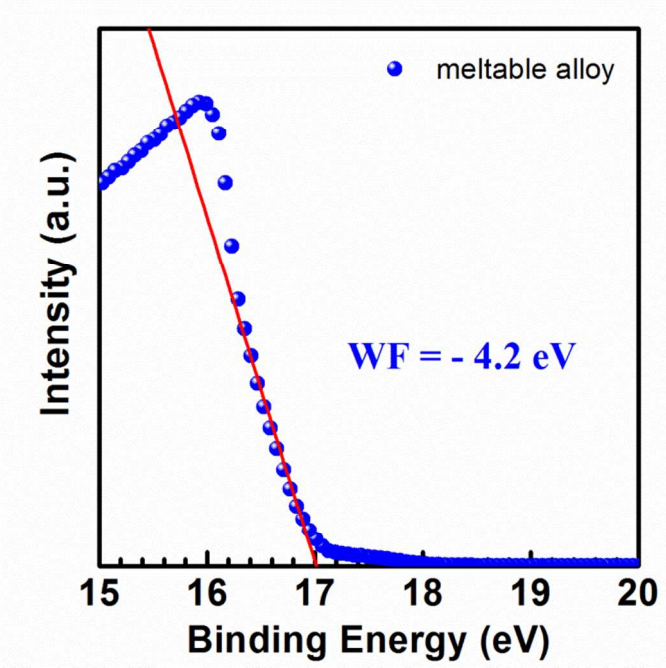

Figure S7. UPS plot for meltable alloy (blue circles) and linear fit (red solid line).

V. Space Charge Limited Current (SCLC) mobility measurement.

The ambipolar nature of OIP with balanced charge transport was established using SCLC mobility measurement. The electron only device was composed of ITO/TiO_2/OIP/N2200/Alloy while the hole only device was composed of ITO/PEDOT:PSS/OIP/PTB7/Au. The average mobility for hole and electron was $\approx 10^{-2}$ cm^2/V.s, J vs. V and SCLC fit is shown in figure S8.

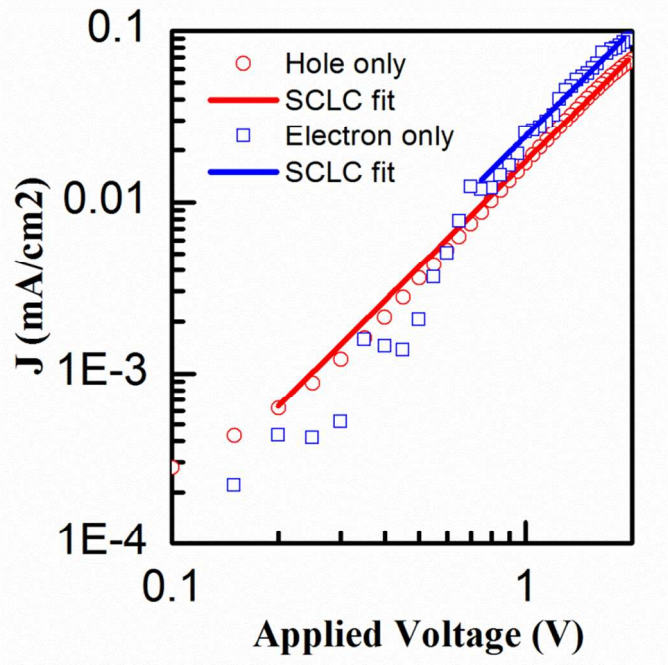

Figure S8. J vs. V plot for electron only device (blue square) and hole only device (red circle). SCLC fit is shown as solid line for electron (blue) and hole (red).

VI. External quantum efficiency

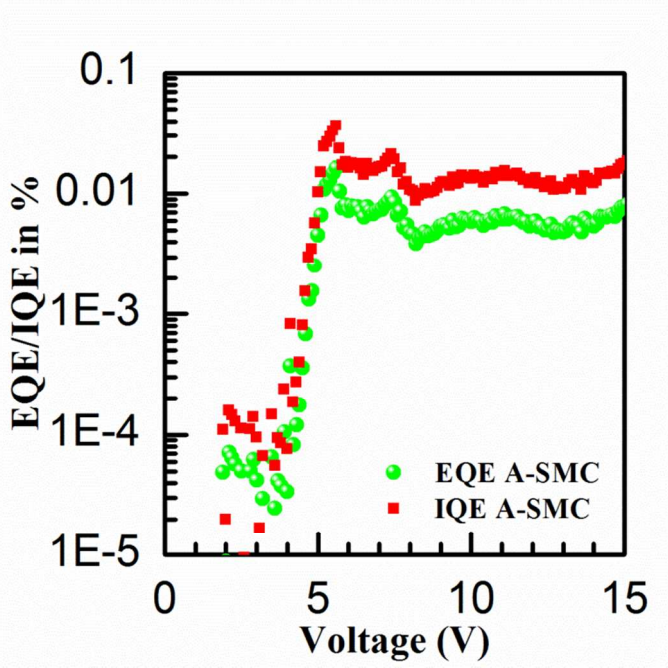

Figure S9: EQE/IQE vs. voltage plot for A-SMC based printable LED.